Electronic Supplementary Material (ESI) for Physical Chemistry Chemical Physics.

Supporting Information

1. Raman spectroscopy and AFM imaging

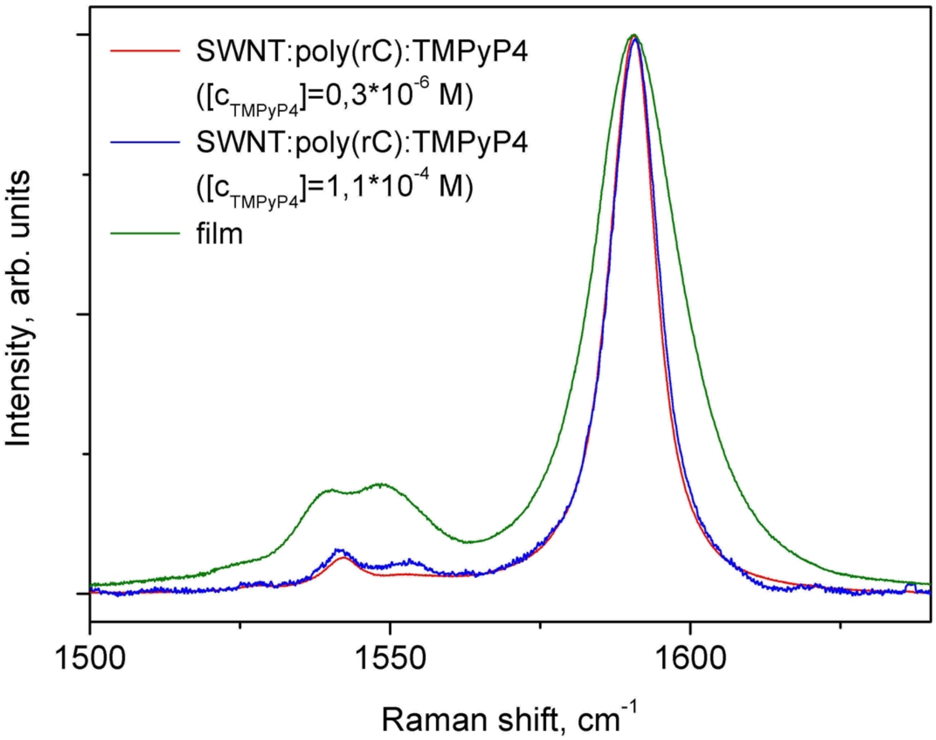

Figure 1S. Raman spectra of SWNT-poly(rC)-TMPyP4 at [c$_{TMPyP4}$]=0.3*10^{-6} M (red line), and [c$_{TMPyP4}$]=1.1*10^{-4} M (blue line) in aqueous suspensions and film (green line) prepared from similar suspension at [c$_{TMPyP4}$]=2*10^{-5} M.

Addition of TMPyP4 into aqueous suspension of SWNT-poly(rC) in the concentration range from 0.33*10^{-6} M to 1.11*10^{-4} M accompanies with small broadening of G^{+} sub-band by ~0.5 cm^{-1} and increasing of ratio of I$_{G-}$/I$_{G+}$ from 6.9 % to 12.6 % where I$_{G-}$ and I$_{G+}$. are the areas under G^{-} (centered at 1542 cm^{-1}) and G^{+} (centered at 1590.5 cm^{-1}) sub-bands respectively . The shape of the G^{-} sub-band is usually attributed to the presence of metallic nanotubes [1]. In SWNT-poly(rC)-TMPyP4 film this trend becomes more pronounced: G^+ band is red-shifted by ~2.2 cm^{-1} and widened by ~8 cm^{-1}, while I_{G-}/I_{G+} ratio is enhanced up to 17.7 %

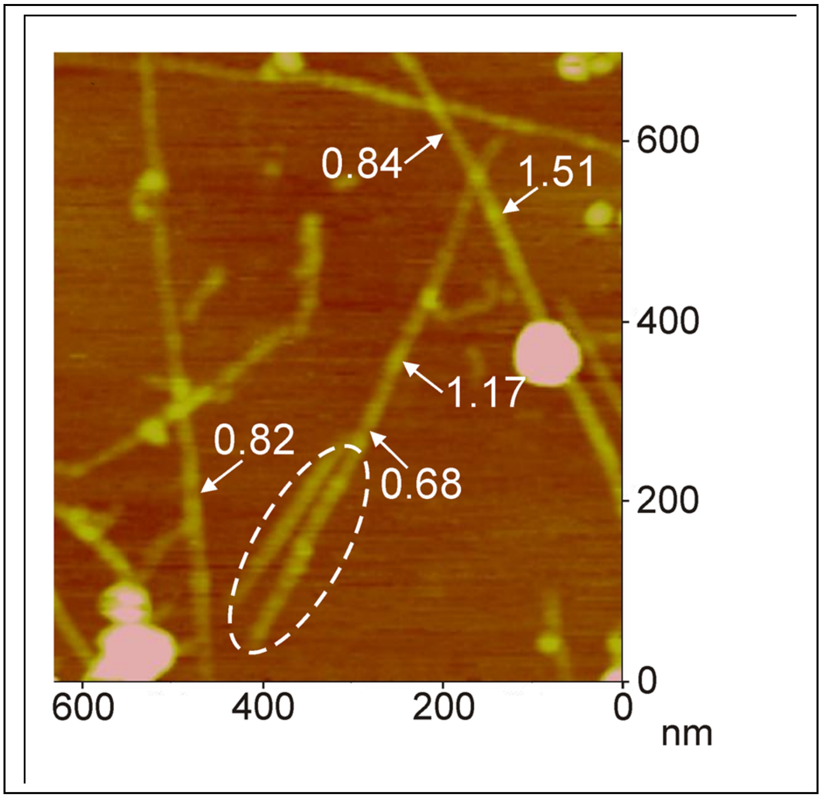

Figure 2S. AFM image of individual and aggregated SWNTs with adsorbed poly(rC). Numbers indicate thickness (height in nm) of nanotubes with (1.17 and 1.51 nm) or without (0.68, 0.82, 0.84 nm) adsorbed polymer. Dotted ellipse shows the dimer formed between two polymer wrapped nanotubes at the beginning of aggregation at low TMPyP4 concentration ($0.3*10^{-6}$ M, in aqueous suspension of SWNT-poly(rC)).

The AFM image (Fig.2S) shows individual nanotubes with the poly(rC) bulges along the nanotube (numbers of which are less than 1 nm indicate the nanotube height without the polymer). It can be seen that some segments of the nanotube surface without polymers. Polymer layers have a certain height distribution which is explained with a peculiarity of adsorption of relatively long biopolymer [2,3]. Small addition of TMPyP4 molecules ($0.3*10^{-6}$ M) into aqueous suspension leads to aggregation of individual polymer-wrapped nanotubes into self assembly as shown in Fig.2S (dimer inside dotted ellipse) .

2. Simulating algorithm

The simulation algorithm comprised of three major sections: (i) preparation of initial setup; (ii) aggregates formation governed by the fusion criterion and (iii) computation of photoluminescence for each type of semiconducting nanotubes ($j=1,2,3,4$ see Table 1 in the main text) distributed over all aggregates followed by statistical averaging. Each averaging was carried out over 200 trials at constant relative concentration C (is average amount of TMPyP4 molecules per nanotube), in the range of three orders of magnitude. Thus, computed $R_j(C)$ dependencies (Eq. (3) in the main text) can be compared with experimental data.

2.1. Initial setup

The simulation has been performed for three dimensional array of $10•10•10$ comprised from $N=1000$ elements. Computational results were not affected by the change of the array size from 8^3 to 12^3. Initially each element was randomly populated by one nanotube of type j ($j=0, 1,2,3,4$; $j=0$ corresponds to the metallic tube) according to probabilities calculated from experimental data for semiconducting tubes ($i=1,2,3,4$) and CoMoCat data sheet for metallic tubes[4] (Table 1 in the main text). Then $C*N$ TMPyP4 molecules were randomly distributed over N elements. Thus, prior simulation (initial setup) each element of the array contains one nanotubes, $n_t=1$, and some amount of TMPyP4 molecules, n_c, which could be a zero.

2.2. Aggregate formation and fusion criterion

The section of algorithm responsible for the aggregates formation consists of two cyclic procedures providing combinatorial analysis of element pairs from *N* manifold (name them as object *A* with coordinates (x,y,z) and as the object *B* with coordinates (x_1, y_1, z_1)) . The external procedure defines the maximal radius R_Δ around object *A* and R_Δ variation in the range of $1 \leq R_\Delta \leq N^{1/3}$, while the internal procedure (inserted into external one) varies the radius ρ with the step of unity in the range of $1 \leq \rho \leq R_\Delta$. In the internal cycle for each ρ, the search of objects *B* is performed satisfying condition: $\rho^2 = dX^2 + dY^2 + dZ^2$, where $X = x - x_1$; $Y = y\text{-}y_1$; $Z = z\text{-}z_1$. Note, that at each step algorithm runs the search of objects *B* around all non-empty objects *A*. For example, for $\rho = 1$ $R_\Delta = 1$ the object *A* (single nanotube) can be fused with object *B* (single nanotube), which is the nearest neighbor to form a dimer. Next , for $R=2$ and $\rho = 1$ the object *A* can be fused with nearest neighbors *B* which are dimers or individual tubes, for $R=2$ and $\rho = 2$ objects *B* can be only individual tubes from the next neighbor layer, etc. As soon as fusion criterion is fulfilled, the number of nanotubes and TMPyP4 molecules (from *A* and *B* objects) are summed in a new object *A* with the same coordinates and the object *B* becomes empty. Thus, the computational algorithm simulates an evolution of the aggregates formation where key parameters are number of TMPyP4 molecules per SWNT-poly(rC) complex and fusion criterion.

For simplicity the orientation factor of SWNT-poly(rC) complexes forming the aggregate was excluded in simulative algorithm. It means that all nanotubes in aggregate stitched by TMPYP4 molecules are parallel each to other that is supported by previous results obtained by molecular dynamics simulation[5]. Also, the constant lengths for all tubes were considered. Model parameter C_m (which is proportional tube lengths) determines the minimal number of TMPYP4 molecules required to fuse two individual SWNT-poly(rC) complexes in one dimer (aggregate comprised of two tubes). As the tube length is not defined, parameter C_m can be selected randomly as a scaling factor, however the real parameter affecting the calculation results is C/Cm ratio.

Chronologically the first fusion criteria (FC) applied to aggregates formation were formulated without accounting of active molecules distributed over the contact area as it is described in the main text (see also therein the definition of C_c and C_p parameters) . In such simple case it was supposed that number of TMPyP4 molecules required to build a stable aggregate should be proportional to the number of nanotubes in two fused aggregates resulting in conditions:

$$C_c = n_{c1} + n_{c2} \geq C_p = C_m(n_{t1} + n_{t2} - 1) \tag{1S}$$

for planar/extended aggregate (one new bond after fusion) and

$$C_c = n_{c1} + n_{c2} \geq C_p = C_m(2(n_{t1} + n_{t2}) - 3) \tag{2S}$$

for small compact aggregate (two new bonds after fusion). However, to satisfy experimental results the above criteria cannot provide any reasonable range of relative concentration change. Figure 3S (a,b) demonstrates $R_i(C)$ dependencies simulated with FCs corresponding Eq.(1S) and Eq.(2S).

In addition, we tried to simulate an aggregate fusion determined by the expression:

$$C_c = n_{c1} + n_{c2} \geq C_p = \frac{1}{2} C_m(n_{t1} + n_{t2})(n_{t1} + n_{t2} - 1) \tag{3S}$$

In this case the minimal amount of TMPyP4 molecules required for fusion of two objects depends roughly on the square of the total number of tubes. The results demonstrate better similarity with experimental data , however still cannot satisfy an observed concentration range of $R_j\ (C)$ reduction and cannot reproduces step-like behavior in experimental $R_j\ (C)$ dependencies (Fig. 3S c)

Meanwhile the use of the criterion accounting active TMPyP4 molecules in the contact area (see Eq. (2) in the main text) allows to achieve a good agreement with experiment.

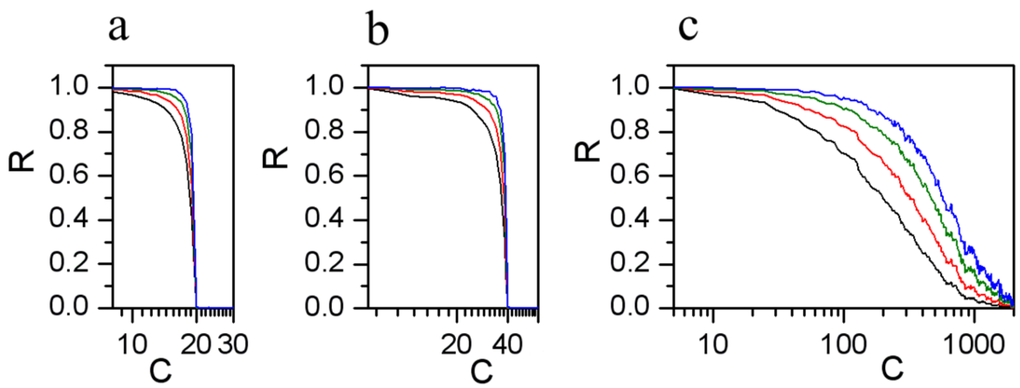

Figure 3S. ***R_j (C)* dependencies simulated for three fusion criteria according to Eq.(1S) – (a), Eq. (2S) – (b) and Eq. (3S) – (c) at parameters *Z_0=0.03 (the part of metallic nanotubes), C_m=20, V_{ij}=V_0=3, η=0.01*. Colors legend corresponding to the type of semiconducting SWNTs (see table 1 for indices *j*): black – *j*=4; red –*j*=3; green- *j*=2; blue – *j*=1**

For estimation of the surface density of TMPyP4 active molecules, it is supposed that aggregate cross-section has a round shape. Then the ρ value presents the upper limit as any deviation from the round shape should increase the surface area and consequently reduce the surface density of TMPyP4 molecules. Especially in the case of small *Nk* values aggregate cannot be considered as a circular cylinder. For example for *Nk* = 2 (when error is largest in due to discrepancy between real and round shape) we can roughly assume that about ¾ surface of each nanotube is accessible for the active TMPyP4 molecules (see Fig. 6). This means that the ρ value, approximately about in $3/(2^{1.5}) = 1.06$ larger than the real surface density. For *Nk* > 2 this error will be even smaller. Therefore, the case of small *Nk* at ρ calculation cannot significantly affect the modeling results.

2.3. Calculation of photoluminescence intensity

The luminescence intensity, $I^{(A)}_j$, of nanotube of type ***j*** in aggregate ***A*** (without metal SWNT) can be derived from the standard system of four balance equations:

$$I_j^{(A)} = \frac{K_j^r}{D_j}(\varepsilon_j + \sum_{i>j}^{4} \varepsilon_i q_i G_{ji} + \sum_{i>p>j}^{4} \sum_{p>j}^{4} \varepsilon_i q_i q_p G_{ip} G_{pj} + M) \tag{4S}$$

where $M = q_4*q_3*q_2*G_{43}*G_{32}*G_{21}$ *for* $j=1$ *and* $M = 0$ *for* $j > 1$;

$G_{ji} = \frac{K_{ji}}{D_j}$ is the probability of the energy transfer between tube *j* and tube *i* ;

$D_j = K^r + K^d + \sum_{i=1}^{i<j} q_i K_{ji}$ is the total deactivation rate for tube ; ε - absorption coefficient at excitation wavelengths; K^r is radioactive and K^d is nonradioactive rates of individual nanotube. For simplicity we assume that ε, K^r and K^d are the same for nanotube of all types. Note, that the weak dependency of absorption coefficient on chilaties for studied nanotubes has been reported recently [6], where measured oscillator strengths for E22 transitions were quite similar with deviation in the range of ~ 10%.

K_{ji} is the energy transfer rate from tube ***j*** to tube ***i*** $(i<j)$, and q_i is the number of nanotubes of type ***i*** in the aggregate ***A***. As total PL yield of individual tubes of type ***j*** $I^{(0)}_j = NZ_j \varepsilon \eta = NZ_j \varepsilon/((1+V_d)$, the ratio $R_j(C)$ can be calculated as:

$$R_j(C) = \frac{\sum_j I_j^{(A)}}{I_j^{(0)}} \tag{5S}$$

where Σ_j means summation over all aggregates without metallic tubes and with tubes of ***j*** type at concentration of C of TMPyP4 molecules. Taking into account $V_d = K^d/K^r = (1-\eta)/\eta$, where η is quantum yield of individual nanotube-poly(rC) complex; $V_{ji} = K_{ji}/K^r$ $(i<j)$, $V_0 = K_{ji}/K^r$ $(i=j)$; and substitute Eq. (4S) into Eq.(5S), a Eq.(3) in the main text can be derived.

2.4. Calculation of $R_j(C)$ functions taking into account spectral overlapping

In Förster theory of the resonance energy transfer the energy transfer rate between the donor (tube *j)* and the acceptor (tube *i*) can be expressed as:

$$K_{ji} = \frac{A}{r^6}\int_0^{\infty}\frac{\varepsilon_i(\nu)F_j(\nu)}{\nu^4}d\nu \qquad (6S)$$

where $\varepsilon_i(\nu)$ and $F_{(j)}(\nu)$ are spectra of absorbance and fluorescence of acceptor and donor respectively; *r* - is the distance between them and *A* is the constant depending on the nature and geometry of donor-acceptor pair. The $1/\nu^4$ factor in Eq.(6S) can be omitted because of the narrow range of the change for wavenumbers (ν), and no distance dependence was taken into account (see main text). Assuming Lorentzian shape and the same line width for each spectral band of four semiconducting tubes, the expression for V_{ji} can be written as:

$$V_{ij} = \frac{K_{ij}}{K^r} = \frac{2V_0}{\pi}\int_{-\infty}^{\infty}\frac{dx}{(1+(\mathrm{X_i}-\mathrm{x})^2)(1+(\mathrm{X_j}-\mathrm{x})^2)} \qquad (7S)$$

where $X_i = 2E_i / W$ and W is the FWHM (full width at half maximum) of spectral bands (the variable model parameter, which is equal for all types of tubes) . Figure 4S shows simulated $R_j(C)$ functions, for several values of parameter W taken from spectra deconvolution (the reasonable range is 0.01 - 0.06 eV), which cannot be adequately fit to our experimental results because of violation condition of $R_4<R_3<R_2<R_1$. Thus, inconsistency of the model with experiment has a qualitative character. Only significant band broadening (more that 0.4 eV, which is no realistic) could provide a consistency with experimental PL quenching. Note, that such broad FWHM result in almost absence of dependence of V_{ji} on wavenumber (ν), and somehow additionally support our first approximation when $V_{ji} = V_0$ for all types of tubes.

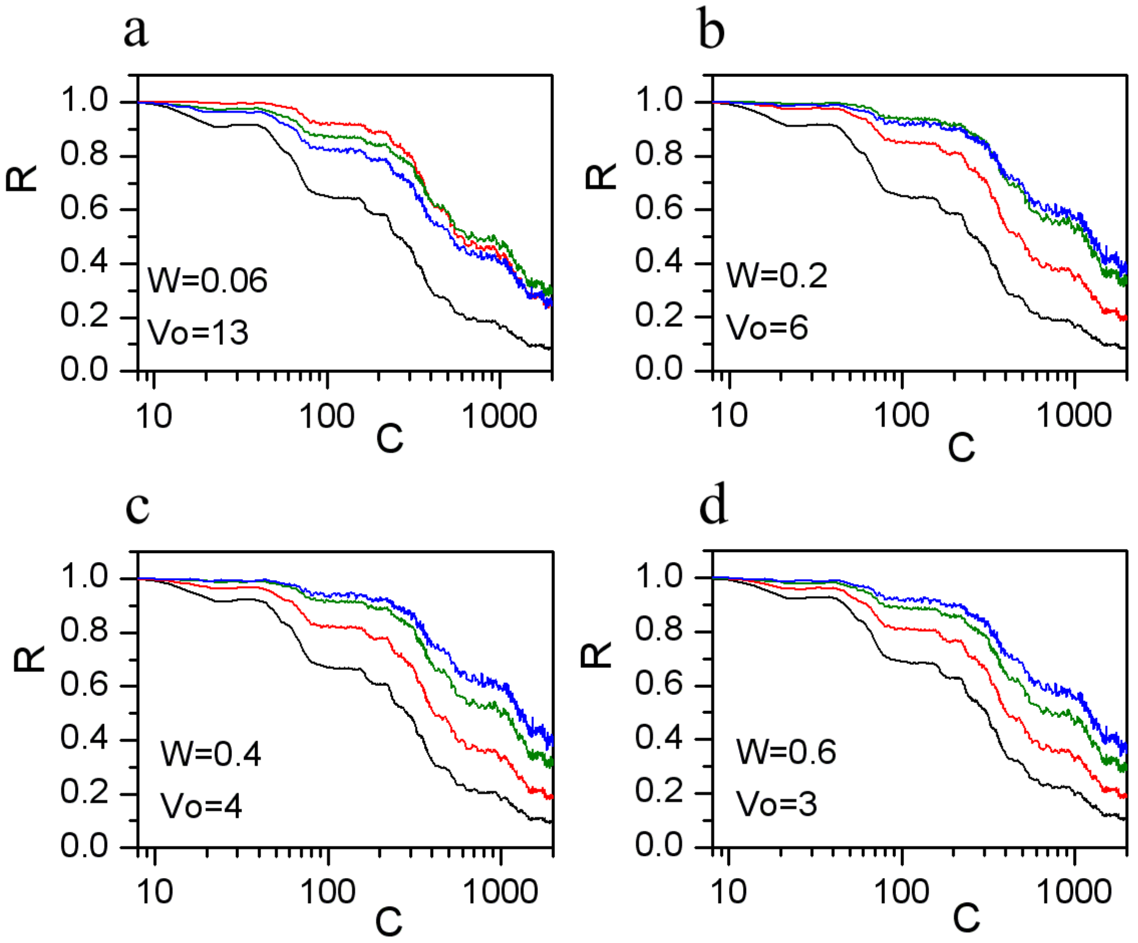

Figure 4S. $R_j(C)$ **functions calculated for** $H=0.7$, $Z_0=0.03$, $\eta=0.01$ **and various W (eV) values. The legend of colors is the same as in Figure 3 (main text) and Figure 3S. The** V_{ij} **values calculated according to Eq.(7S) for:**

a- W=0.06 eV, $V_0=13.00$ $V_{12}=2.09$ $V_{13}=0.77$ $V_{14}=0.54$ $V_{23}=3.34$ $V_{24}=1.75$ $V_{34}=7.67$

b- W=0.2 eV, $V_0=6.00$ $V_{12}=4.08$ $V_{13}=2.47$ $V_{14}=1.94$ $V_{23}=4.76$ $V_{24}=3.80$ $V_{34}=5.65$

c - W=0.4 eV, $V_0=4.00$ $V_{12}=3.58$ $V_{13}=2.95$ $V_{14}=2.63$ $V_{23}=3.76$ $V_{24}=3.50$ $V_{34}=3.94$

d - W=0.6 eV, $V_0=3.00$ $V_{12}=2.85$ $V_{13}=2.59$ $V_{14}=2.44$ $V_{23}=2.92$ $V_{24}=2.82$ $V_{34}=2.98$

References

1. S. D. M. Brown, A. Jorio, P. Corio, M. S. Dresselhaus, G. Dresselhaus, R Saito and K. Kneipp Phys. Rev. B (2001) **63,** 155414.

2. M.V. Karachevtsev, O.S. Lytvyn, S.G. Stepanian, V.S. Leontiev, L. Adamowicz, V.A. Karachevtsev, J. Nanosci. Nanotechnol. (2008) **8**, 1473.
3. T. Hayashida, K. Umemura, Colloids Surf. B (2013) **101**, 49.
4. http://swentnano.com/tech/docs/TD_SG65i.pdf
5. E. S. Zarudnev, A. M. Plokhotnichenko, V. S. Leontiev, I. A. Levitsky, V. A. Karachevtsev J. Material Chemistry (2012) **22**, 10795-10804
6. J. K. Streit , S. M. Bachilo , S. Ghosh , C-W Lin , and R. B. Weisman, Nano Letters (2014) **14**, 1530-1536